

Mechanical properties and differentiation assessments of neural stem cells with pneumatic micropipette aspiration

Ming Wu^{1,4}, Qili Zhao², Cui Yang³, Wen Shen³, Xin Zhao^{2,*}, Yun Lu^{3,*} and Xi Zeng Feng^{1,*}

¹State Key Laboratory of Medicinal Chemical Biology, College of Life Science, and

²Tianjin Key Laboratory of Intelligent Robotics, Nankai University, Tianjin 300071, China

³TEDA Hospital, No. 65 Third Avenue, Economic-Technological Development Area, Tianjin 300457, China

⁴College of Life Sciences, Qufu Normal University, Qufu 273165, China

The change in chemical and biological properties of neural stem cells (NSCs) before and after differentiating into neurons and glial cells has been well studied. However, there is lack of knowledge on the relationship between cell differentiation and alteration of cell mechanical features. Mechanical properties can reflect specific changes that occur with biochemical and cytological changes. Here, we present a robotic micromanipulation system for measuring the mechanical properties of single cells. This system consists of a suction micropipette, a robotic micromanipulator and an inverted microscope. A pneumatic micropipette aspiration method is utilized to measure the elastic properties of the cells. We found that the mechanical properties of NSCs belong to the solid state, however, neurons and glial cells are close to the liquid state. Further, NSCs are harder than neurons and glial cells.

Keywords: Mechanical properties, robotic micromanipulation system, differentiation assessment, neural stem cells.

NEURAL stem cells (NSCs) isolated from embryonic culture as neurospheres can differentiate into neurons, astrocytes and oligodendrocytes¹. NSCs and neurally differentiated cells are good models for studying cellular mechanism for the treatment of nervous system diseases^{2,3}, such as spinal cord injury^{4,5}, Parkinson's disease^{6,7} and Alzheimer's disease^{8,9}. At present, there is lack of data on the mechanical features of NSCs because the current research is focused on biochemical¹⁰ and electrophysiological aspects¹¹. Mechanical properties of single cells reflect specific changes along with differentiation¹². Research on living cell mechanics helps explore cell structure and function^{13–15}, probe the mechanism of developmental process of embryos¹⁶ and investigate disease mechanisms and progression¹⁷. Therefore, it has received a lot of attention in the past few years. Recently,

the mechanical properties of adipose-derived mesenchymal stem cells (MSCs) were found to be correlated with their abilities to produce tissue-specific metabolites¹⁸. From this work, a series of mechanical parameters obtained using the atomic force microscope (AFM) have been proved to be mechanical biomarkers for different MSC types.

The traditional devices for measuring the mechanical properties of cells include the AFM^{19,20}, optical trap (laser tweezers)^{21,22}, plane and micropipette equipped micro-force sensor^{23,24}, microfluidic devices^{25–27} and suction micropipette^{28,29}. Among them, the suction aspirated micropipette has a significantly wider pressure range, a relatively shorter operating time, and advantages that are independent of special or expensive equipment, hence, it has been widely used in such studies. In this method, a suction micropipette is controlled to contact a cell and a negative pressure is applied to deform it, elongating a portion of the cell into the micropipette. The cell deformation images are recorded using a camera and the cell mechanical parameters are derived through the relationship between cell deformation and the negative pressure.

In the micropipette aspiration process, negative pressure is applied by a liquid fluid reservoir which creates fine pressure steps through precise control of height of the liquid in the reservoir²⁸. However, as evaporation of liquid in the reservoir continues, the liquid level in the reservoir usually drops and causes a drift of negative exerted pressure. This requires the operator to frequently adjust the height of the manipulator which increases the operation challenge and potentially reduces the precise derived results. This disadvantage can be eliminated by replacing the device with a pneumatic-driven injection. However, the negative pressure generated by the equipped vacuum generator is susceptible to fluctuations, and it is difficult to keep the negative pressure in a suitable state required by suction of cells. Further, the capillary effect between the micropipette and the injection micropipette (IM) has a significant effect on the suction pressure during micropipette aspiration.

The aim of this study is to introduce a method to measure the mechanical properties of NSCs using a commercially available pneumatic-driven injector. With this approach, we can observe the differentiation of NSCs in a simple, accurate and cost-effective manner. During the suction process, the system provides positive pressure that can be more precisely controlled than negative pressure to neutralize the capillary action effect and produce a small negative pressure on the NSCs. The magnitude of the imposed negative pressure on the cells is calculated according to the balanced pressure model.

NSCs were isolated and purified from E18 SD rat hippocampus and propagated as previously described³⁰. Briefly, the tissue was mechanically dissociated and cultured in DMEM/F12 medium (Hyclone, USA)

*For correspondence. (e-mail: zhaoxin@nankai.edu.cn; tedaluyun@163.com; xzfeng@nankai.edu.cn)

supplemented with 2% B27 (Gibco-Invitrogen), 2 mM L-glutamine (Sigma-Aldrich), 1% penicillin/streptomycin (Gibco-Invitrogen), 20 ng/ml epidermal growth factor (Sigma-Aldrich), and 20 ng/ml fibroblast growth factor-2 (Sigma-Aldrich). Half of the medium was replaced with fresh culture medium every 3–4 days. The generated neurospheres were passaged via mechanical dissociation through scratching with a plastic pipette tip. All animal procedures were carried out in accordance with animal-use protocols approved by the Nankai University Animal Care and Use Committee, China.

For serum-induction experiments, passages 3 neurospheres were mechanically dissociated through scratching with a plastic pipette tip and plated into DMEM/F12 medium containing 2% B27, 2 mM L-glutamine, 1% penicillin/streptomycin and 10% of foetal bovine serum (FBS). Under this condition, NSCs can differentiate into mixed line of neurons, astrocytes and oligodendrocytes. Cells were cultured for five days before being processed for imaging, immunocytochemical and micropipette aspiration analysis.

For immunofluorescence staining of NSCs, cells were washed with PBS, fixed with 4% paraformaldehyde at room temperature for 30 min and permeabilized with 0.2% Triton X-100 (TPBS) for 5 min. The cells were then blocked using 5% (v/v) goat serum for 60 min before incubation with primary antibodies overnight at 4°C: nestin (booster, BA1289, 1:1000), GFAP (booster, BA0056, 1:1000), MAP2 (booster, BM1243, 1:1000). After primary antibody incubation, secondary antibodies were incubated for 60 min, followed by 4,6-diamidino-2-phenylindole (DAPI) staining. Samples were examined with fluorescent microscopy (Nikon Ti-U, Japan). For each sample, three images at 10× and 20× magnification were taken at random locations from the slides.

The micropipette aspiration system consists of the following parts (Figure 1): an inverted microscope (CK-40, Olympus), a CCD camera (W-V-460, Panasonic) for microscope image gathering at the speed of 30 frames/s, an in-house developed micro-injector supplying suction pressure with a resolution of 10 Pa, a pair of in-house developed X–Y–Z micromanipulators (with travel range of 50 mm, maximum speed of 2 mm/s and repeatability of ±1 μm) for mounting micropipettes, a X–Y microplatform (with travel range of 100 mm, maximum speed of 2 mm/s and repeatability of ±1 μm) for positioning the petri dish, and a host computer for controlling the above devices, processing and displaying microscope images^{31,32}.

The micropipettes used in the experiments were made from borosilicate glass tubes with an outer diameter of 1 mm and inner diameter of 0.8 mm. The tubes were prepared using a micropipette puller (MODEL P-97 Sutter Instrument) to form long, tiny tips. Then the tips were fractured by a micro-forge (MF-900, NARISHIGE, Japan) to obtain the required diameter (about 10 μm). Further, they were melted on the micro-forge to make the

opening smooth and the micropipette was bent by 45° using the micro-forge and mounted on the manipulators, positioning the tip of IM horizontally.

A droplet of trypsin and two droplets of culture medium were placed in the petri dish separately and covered by paraffin (Figure 1c). Trypsin droplets were used to clean the micropipette to keep the inner surface of the micropipette smooth and ensure the suction operation. The culture medium was used to locate cells and perform micropipette aspiration, as well as for dissolving and removing trypsin when the micropipette was moved back from the trypsin droplet.

When the micropipette is moved into the culture medium, liquid gets filled into it, and cells can be drawn into the micropipette without any other suction pressure; this makes the pneumatic micropipette aspiration operation a difficult one. However, if a positive pressure is applied by the pump to balance the capillary effect, the aspiration pressure at the opening of the micropipette may be controlled quantitatively through accurately changing the positive pressure. Based on this principle, a method to measure mechanical properties of NSCs using a pneumatic micropipette is proposed.

As shown in Figure 2, the gas–liquid interface (GLI) in the micropipette can be maintained in a balanced state by imposing a positive pressure P_1 . Then, by decreasing the positive pressure, part of the cell surface can be pulled into the micropipette and a seal will be formed between the cell and the micropipette. At this moment, GLI is still in an equilibrium state. The forces exerted on it, including the surface tension force f and positive pressure P_1 , maintain balance according to

$$f = P_1 * \pi * R_1^2, \quad (1)$$

where R_1 is the inner radius of the micropipette.

In eq. (1), the surface tension force f , generated by the capillary effect can be derived according to

$$f = 2\pi R_1 \sigma \cos \alpha, \quad (2)$$

where σ is the surface tension coefficient of the culture medium and α is the contacting angle at the GLI.

Combining eqs (1) and (2), P_1 can be derived as

$$P_1 = 2\sigma \cos \alpha / R_1. \quad (3)$$

Decreasing P_1 to $P_1 - \Delta P$, an aspiration pressure ΔP is generated. According to eq. (3), ΔP can be derived as

$$\Delta P = \Delta P_1 + 2\sigma(\cos \alpha' / R_1' - \cos \alpha / R_1), \quad (4)$$

where α' and R_1' are the contacting angle and inner radius of the micropipette at the new position of GLI respectively. We observe that the contacting angle and

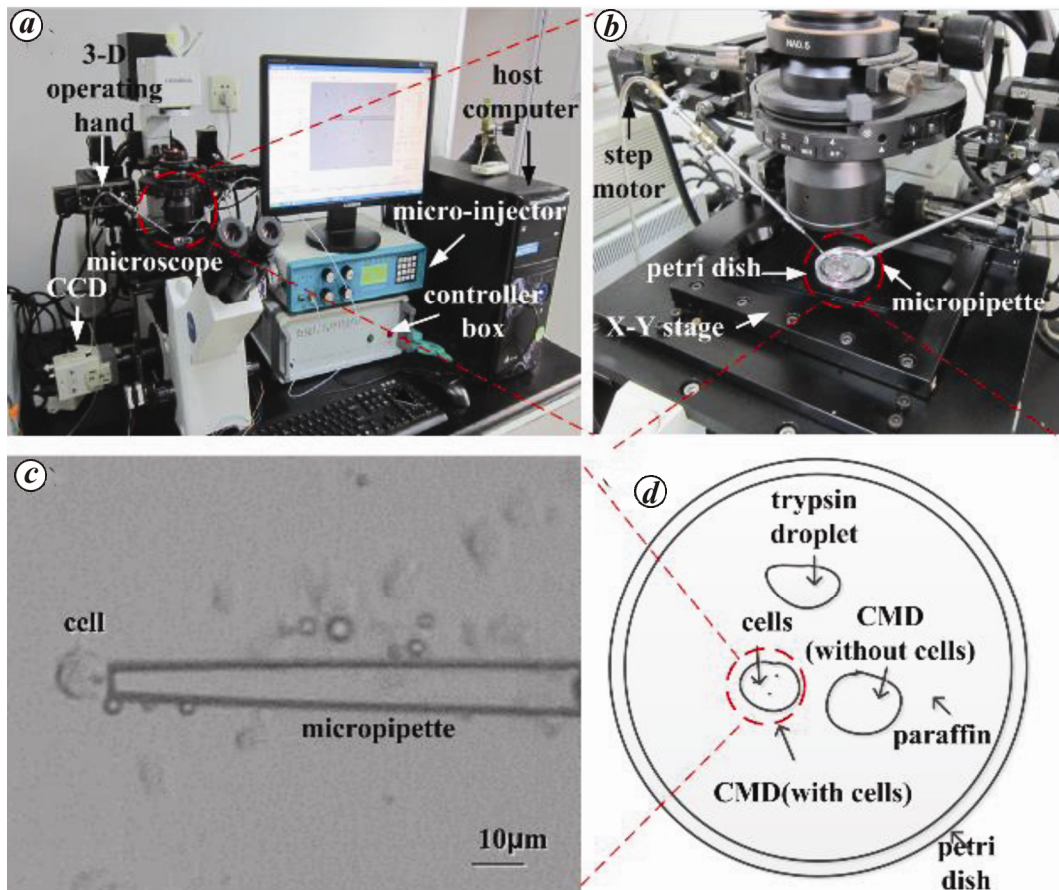


Figure 1. Micropipette aspiration system set-up. *a, b*, Actual set-up of the robotic micropipette aspiration system. *c, d*, Schematic illustration and operation modes of the robotic micromanipulation system to manipulate single cells.

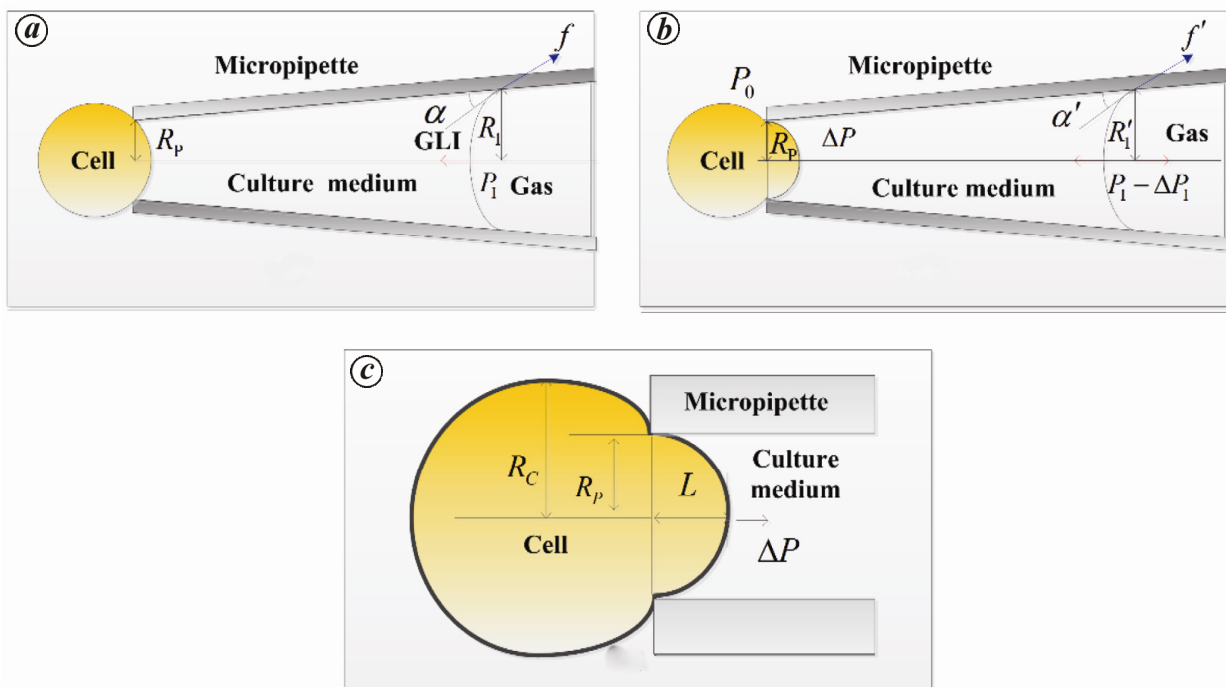


Figure 2. Schematic of the pneumatic micropipette aspiration method: *a*, Seal formation: the seal is formed through reducing positive pressure P_1 . *b*, Aspiration of the cell: by adjusting positive pressure P_1 , the aspiration pressure ΔP at the micropipette opening is quantified. *c*, Shell model of the cell: mechanical properties of the cell can be determined using relationship between aspiration pressure ΔP and projection length L_p .

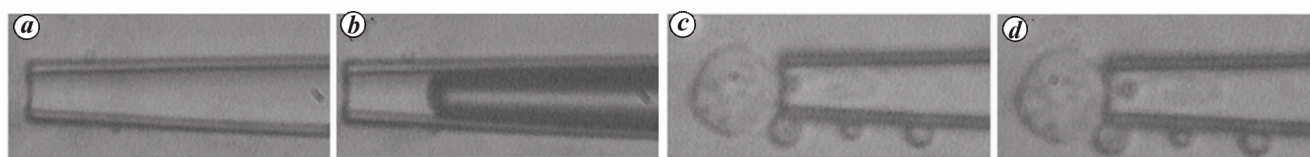


Figure 3. Micropipette aspiration experiments of the cell. *a*, Liquid entering into the micropipette under the capillary effect. *b*, A positive pressure is exerted to pull most of the liquid out of the micropipette. *c*, A seal between the cell and the micropipette is formed through reducing positive pressure. *d*, Decrease the positive pressure to aspirate the cell.

inner radius of the micropipette at the position of GLI are basically kept constant during micropipette aspiration for NSCs. Hence, ΔP can only be determined by the variation of P_1 , which means

$$\Delta P = \Delta P_1. \quad (5)$$

NSCs have very thin cell membranes surrounding their cytoplasm. According to the shell model of the cell, the cytoplasm with different mechanical properties surrounded by the cell membrane can be considered as a solid or a liquid surrounded by the membrane²⁸. The mechanical properties of the solid or liquid-like cells are significantly different. As shown in Figure 2*c*, when a negative pressure is exerted on the cell, it will form a projection with length L_p in the micropipette. The response of the solid or liquid-like cells to the aspiration pressure is similar until L_p is equal to R_p . A further increase of aspiration pressure causes a liquid-like cell to flow completely into the micropipette, whereas for the solid cell, L_p increases linearly with increase in the aspiration pressure²⁸.

Figure 3 shows the procedure for micropipette aspiration experiments on NSCs. First, the micropipette moves down to the culture medium and liquid enters into it under capillary action (Figure 3*a*). Thereafter, a positive injection pressure is applied to push most of the liquid out of the micropipette (Figure 3*b*). Next, the micropipette moves close to a cell and the positive pressure is reduced to pull the cell membrane into the micropipette and form a seal (Figure 3*c*). In addition, the positive pressure is gradually reduced and microscope images of the suction process are captured (Figure 3*d*).

During micropipette aspiration process, the projection length of the cell L_p is derived through the distance between the opening of the micropipette and the rightmost point of the cell surface, both of which are inputted to the system using a computer. The aspiration pressure ΔP is derived from the variation of positive pressure P_1 . In order to improve the control solution of ΔP , P_1 is determined through the open size of the adjusting valve of the pump, which can provide a solution about 0.3 Pa.

The differentiation of rat neural stem cells in different culture media was examined by immunohistochemistry. Lineage-specific differentiation was monitored with markers of NSCs (nestin), astrocytes (GFAP) and neurons

(MAP2). After five days of culture, undifferentiated NSCs formed neurospheres in serum-free medium. These cells showed nest-positive, GFAP-negative and MAP2-negative (Figure 4*a-c*). There were very few differentiated cells in the neurospheres (Supplementary Figure 1). However, after five days of FBS induction, NSCs differentiated into GFAP-positive astrocytes or MAP2-positive neurons (Figure 4*d-i*).

According to the derived L_p and ΔP during the aspiration process, Figure 5 shows the relationship between L_p/R_p and ΔP of the cells before differentiation (BD) and after differentiation (AD). Figure 5*a*, video S1 and video S2 (see Supplementary file online) show the aspiration process under different ΔP values. It can be easily seen that whether $L_p/R_p < 1$ or $L_p/R_p > 1$, here L_p/R_p increases linearly with ΔP for the cells before differentiation, which means the BD cells behave in a solid state. On the contrary, for the cells after differentiation, when $L_p/R_p < 1$, L_p/R_p and ΔP show a linear relationship. When $L_p/R_p > 1$, the cells flow into the micropipette quickly without any increase in ΔP . The results show that, the AD cells behave in a liquid state. According to the slope between L_p/R_p and ΔP , when $L_p/R_p < 1$, the cells become softer after differentiation.

Cell differentiation involves a wide variety of structural reorganization within the nucleus, including chromatin condensation and nucleoprotein immobilization^{33,34}. The alteration of gene expression and protein abundance leads to changes in cytoskeletal structure and architecture³⁵. One possible mechanism by which embryonic stem cells become softer with differentiation is the change in cell nuclear stiffness³³. Stem cells may have similar properties, so we speculate that mechanisms of mechanical changes in NSCs may be similar to embryonic stem cells.

We have developed a robotic micromanipulation approach for measuring cell mechanical properties based on single-cell suction micropipette system. This system uses a pneumatic aspiration method to quantify the aspiration pressure and measure the cell mechanical properties. It consists of a commercial pneumatic driven injector, traditional microscope and manipulators. To obtain neurally differentiated cells, NSCs were cultured in FBS-treated medium. According to the captured microscopic images and the recorded pressures, we obtained the mechanical properties of NSCs before and after differentiation. The

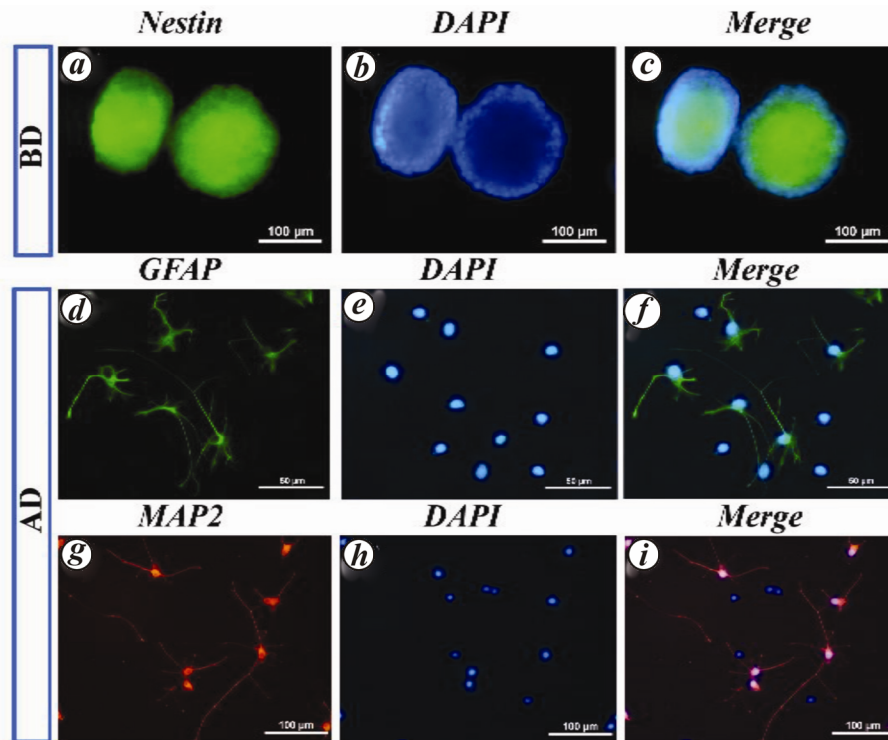


Figure 4. Foetal bovine serum-induced differentiation of neural stem cells. *a–c*, Before differentiation (BD); nestin-positive neural stem cells (NSCs). *d–i*, After differentiation (AD): *d–f*, GFAP-positive astrocytes. *g–i*, MAP2-positive neurons.

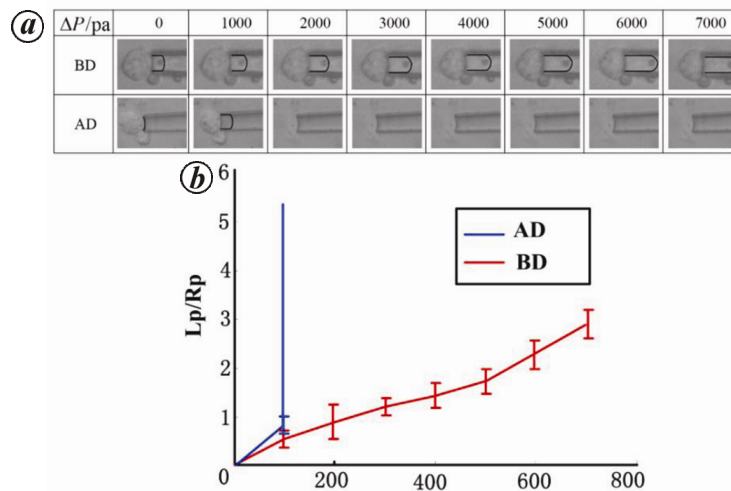


Figure 5. Results of the micropipette aspiration experiments on NSCs. *a*, The derived projection length L_p of NSCs before differentiation (BD) and after differentiation (AD) under different aspiration pressures ΔP . *b*, Relationship between ΔP and L_p of NSCs before differentiation and after differentiation. Twenty cells were measured in each group.

data demonstrate that after NSCs differentiate into neurons or glial cells, the Young's modulus decreases. The molecular aspects regarding change in mechanical properties merit further studies for biological applications. Thus, based on the present study, we can observe the differentiation of NSCs without immunocytochemistry in the future.

Conflict of interest: The authors declare that they have no conflicts of interest.

1. Gage, F. H., Mammalian neural stem cells. *Science*, 2000, **287**, 1433–1438.
2. Ming, G.-L. and Song, H., Adult neurogenesis in the mammalian brain: significant answers and significant questions. *Neuron*, 2011, **70**, 687–702.

3. Sloan, S. A. and Barres, B. A., Mechanisms of astrocyte development and their contributions to neurodevelopmental disorders. *Curr. Opin. Neurobiol.*, 2014, **27**, 75–81.
4. Chu, T., Zhou, H., Li, F., Wang, T., Lu, L. and Feng, S., Astrocyte transplantation for spinal cord injury: current status and perspective. *Brain Res. Bull.*, 2014, **107**, 18–30.
5. Ponemone, V., Choudhury, K., Harris, K. L. and Dewan, Y., Stem cell treatment for the spinal cord injury – a concise review. *Indian J. Neurotrauma*, 2014, **11**, 30–38.
6. Freed, J. W. *et al.*, Human embryonic stem cells, dopaminergic neurons, and pathways for developing a Parkinson's disease therapy. In *Cellular Transplantation* (eds Halberstadt, C. and Emerich, D.), Academic Press, Burlington, 2007, pp. 523–IX.
7. Foster, H. D. and Hoffer, A., Hydroxylation of the two catecholamines, dopamine and adrenaline: Implications for the etiologies and treatment of encephalitis lethargica, Parkinson's disease, multiple sclerosis, amyotrophic lateral sclerosis, and schizophrenia. In *Oxidative Stress and Neurodegenerative Disorders* (eds Qureshi, G. A. and Parvez, S. H.), Elsevier Science B.V., Amsterdam, pp. 369–382.
8. Vazin, T. *et al.*, Efficient derivation of cortical glutamatergic neurons from human pluripotent stem cells: a model system to study neurotoxicity in Alzheimer's disease. *Neurobiol. Dis.*, 2014, **62**, 62–72.
9. Forlenza, O. V., De-Paula, V. J. R. and Diniz, B. S. O., Neuroprotective effects of lithium: implications for the treatment of Alzheimer's disease and related neurodegenerative disorders. *ACS Chem. Neurosci.*, 2014, **5**, 443–450.
10. Chen, Y., Aardema, J. and Corey, S. J., Biochemical and functional significance of f-bar domain proteins interaction with WASP/N-WASP. *Semin. Cell Dev. Biol.*, 2013, **24**, 280–286.
11. Muñoz, F., Reales, J.M., Sebastián, M. Á. and Ballesteros, S., An electrophysiological study of haptic roughness: effects of levels of texture and stimulus uncertainty in the p300. *Brain Res.*, 2014, **1562**, 59–68.
12. Darling, E. M., Topel, M., Zauscher, S., Vail, T. P. and Guilak, F., Viscoelastic properties of human mesenchymally-derived stem cells and primary osteoblasts, chondrocytes, and adipocytes. *J. Biomech.*, 2008, **41**, 454–464.
13. Fletcher, D. A. and Mullins, R. D., Cell mechanics and the cytoskeleton. *Nature*, 2010, **463**, 485–492.
14. Lu, Y.-B. *et al.*, Viscoelastic properties of individual glial cells and neurons in the CNS. *Proc. Natl. Acad. Sci.*, 2006, **103**, 17759–17764.
15. Dingal, P. C. D. P. and Discher, D. E., Material control of stem cell differentiation: challenges in nano-characterization. *Curr. Opin. Biotech.*, 2014, **28**, 46–50.
16. Heisenberg, C.-P. and Bellaïche, Y., Forces in tissue morphogenesis and patterning. *Cell*, 2013, **153**, 948–962.
17. Suki, B. *et al.*, Mechanical failure, stress redistribution, elastase activity and binding site availability on elastin during the progression of emphysema. *Pulm. Pharmacol. Ther.*, 2012, **25**, 268–275.
18. González-Cruz, R. D., Fonseca, V. C. and Darling, E. M., Cellular mechanical properties reflect the differentiation potential of adipose-derived mesenchymal stem cells. *Proc. Natl. Acad. Sci. USA*, 2012, **109**, E1523–E1529.
19. Sato, M., Nagayama, K., Kataoka, N., Sasaki, M. and Hane, K., Local mechanical properties measured by atomic force microscopy for cultured bovine endothelial cells exposed to shear stress. *J. Biomech.*, 2000, **33**, 127–135.
20. Wu, H. W., Kuhn, T. and Moy, V. T., Mechanical properties of 1929 cells measured by atomic force microscopy: effects of anti-cytoskeletal drugs and membrane crosslinking. *Scanning*, 1998, **20**, 389–397.
21. Dai, J. and Sheetz, M. P., Mechanical properties of neuronal growth cone membranes studied by tether formation with laser optical tweezers. *Biophys. J.*, 1995, **68**, 988–996.
22. Laurent, V. M., Hénon, S., Planus, E., Fodil, R., Balland, M., Isabey, D. and Gallet, F., Assessment of mechanical properties of adherent living cells by bead micromanipulation: comparison of magnetic twisting cytometry vs optical tweezers. *J. Biomech. Eng.*, 2002, **124**, 408–421.
23. Sun, Y. and Nelson, B. J., MEMS capacitive force sensors for cellular and flight biomechanics. *Biomed. Mater.*, 2007, **2**, S16–S22.
24. Yang, S. and Saif, M. T. A., MEMS based force sensors for the study of indentation response of single living cells. *Sensors Actuat. A*, 2007, **135**, 16–22.
25. Hochmuth, R. M., Micropipette aspiration of living cells. *J. Biomech.*, 2000, **33**, 15–22.
26. Haider, M. A. and Guilak, F., An axisymmetric boundary integral model for assessing elastic cell properties in the micropipette aspiration contact problem. *J. Biomech. Eng.*, 2002, **124**, 586–595.
27. Palmer, T. D., Takahashi, J. and Gage, F. H., The adult rat hippocampus contains primordial neural stem cells. *Mol. Cell Neurosci.*, 1997, **8**, 389–404.
28. Hsieh, J., Aimone, J. B., Kaspar, B. K., Kuwabara, T., Nakashima, K. and Gage, F. H., IGF-I instructs multipotent adult neural progenitor cells to become oligodendrocytes. *J. Cell Biol.*, 2004, **164**, 111–122.
29. Zhao, Q. *et al.*, A novel pneumatic micropipette aspiration method using a balance pressure model. *Rev. Sci. Instrum.*, 2013, **84**, 123703.
30. Kaech, S. and Banker, G., Culturing hippocampal neurons. *Nature Protoc.*, 2006, **1**, 2406–2415.
31. Zhao, Q., Sun, M., Cui, M., Yu, J., Qin, Y. and Zhao, X., Robotic cell rotation based on the minimum rotation force. *IEEE Trans. Automat. Sci. Eng.*, 2015, **12**, 1504–1515.
32. Zhao, Q., Shirinzadeh, B., Cui, M., Sun, M., Liu, Y. and Zhao, X., A novel cell weighing method based on the minimum immobilization pressure for biological applications. *J. Appl. Phys.*, 2015, **118**, 044301.
33. Pajerowski, J. D., Dahl, K. N., Zhong, F. L., Sammak, P. J. and Discher, D. E., Physical plasticity of the nucleus in stem cell differentiation. *Proc. Natl. Acad. Sci. USA*, 2007, **104**, 15619–15624.
34. Duncan, E. M., Muratore-Schroeder, T. L., Cook, R. G., Garcia, B. A., Shabanowitz, J., Hunt, D. F. and Allis, C. D., Cathepsin I proteolytically processes histone H3 during mouse embryonic stem cell differentiation. *Cell*, 2008, **135**, 284–294.
35. Darling, E. M. and Di Carlo, D., High-throughput assessment of cellular mechanical properties. *Annu. Rev. Biomed. Eng.*, 2015, **17**, 35–62.

ACKNOWLEDGEMENTS. This project was initiated in the State Key Laboratory of Medicinal Chemical Biology at Nankai University, China. X.Z. and X.Z.F. were supported by the Special Fund for Basic Research on Scientific Instruments of the Chinese National Natural Science Foundation (Grant No. 61327802). Y.L. was supported by the Tianjin Science Technology Research Funds of China (Grant No. F1012921). We thank the Shandong Province–Youth Fund Project: ZR2016HQ32 and the Qufu Normal University fund (xkj201510).

Received 13 June 2017; revised accepted 5 December 2017

doi: 10.18520/cs/v114/i09/1961-1966